New findings on hurricane intensity, wind field extent, and surface drag coefficient behavior

Mark D. Powell
NOAA Atlantic Oceanographic and Meteorological Laboratories
 Hurricane Research Division
Miami FL 33149

1. Introduction

Analysis of several years of measurements from relatively new sensors are changing our views of hurricane intensity, the radial extent of the surface wind field, and the behavior of the surface drag coefficient in extreme winds.

2. Hurricane Intensity

Although defined as "the highest one-minute average wind speed (at an elevation of 10 m with an unobstructed exposure) associated with that weather system at a particular point in time", intensity is nearly impossible to measure and provides no consideration of storm size. On the day following Hurricane Katrina's landfall, Mr. Jim Holt of Biloxi MS commented: "It looks like Hurricane Camille killed more people yesterday than it did in 1969." Apparently some personal evacuation and storm preparation decisions were made based on comparing Hurricane Katrina to Hurricane Camille, since both were Saffir-Simpson category five storms a day prior to landfall. People were familiar with the areas that Camille had flooded, and perhaps felt that Katrina was incapable of exceeding Camille's damage, despite warnings of extreme storm surge and waves. Katrina, however was much larger than Camille, greatly increasing it's capacity to inflict damage. Hurricane damage potential, as currently defined by the Saffir-Simpson scale and the maximum sustained surface wind speed in the storm, fails to consider the area impact of winds likely to force surge and waves or cause particular levels of damage. To demonstrate the importance of storm size, we compared the integrated kinetic energy of Hurricanes Camille and Katrina. While both storms achieved Category five status, Katrina on the day before landfall exhibited twice the integrated kinetic energy for winds > hurricane force. At landfall, Katrina weakened to Cat 3 status but the expansion of the wind field allowed the integrated kinetic energy to be maintained at the same level as when a Cat 5, resulting in large losses due to storm surge, wave, and wind damage. When communicating hurricane awareness, it is important not to focus primarily on the Saffir-Simpson Category or storm intensity... the combination of storm size and intensity govern the potential for storm damage. Integrated kinetic energy represents a framework that captures the physical process of ocean surface stress forcing waves and surge while also taking into account structural wind loading and the spatial coverage of the wind. Integrated kinetic energy was computed from gridded, objectively analyzed surface wind fields of 23 hurricanes representing large and small storms.
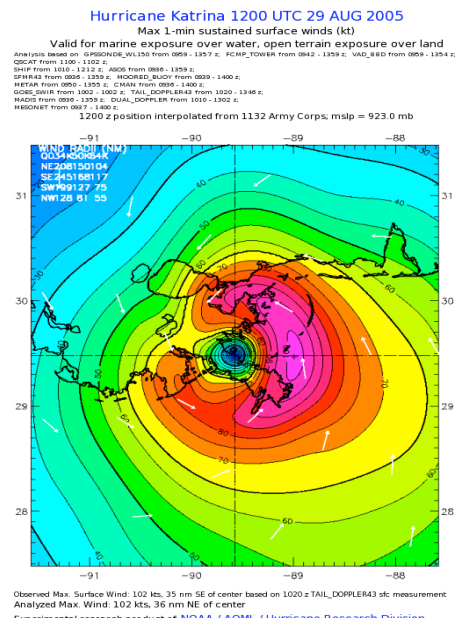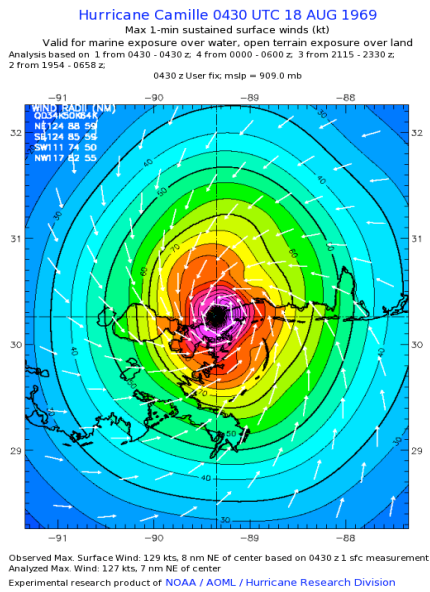
Fig. 1 Wind fields of Hurricanes Camille of 1969 (left) and Katrina of 2005 (right). The integrated kinetic energy contribution by winds > hurricane force is 63 TJ for Camille compared to 122 TJ for Katrina.

A wind destructive potential rating was developed by weighting wind speed threshold contributions to the integrated kinetic energy, based on observed damage in Hurricanes Andrew, Hugo, and Opal. A combined storm surge and wave destructive potential rating was then assigned according to the integrated kinetic energy contributed by winds greater than tropical storm force. The ratings are based on the familiar 1-5 range, with continuous fits to allow for storms as weak as 0.1 or as strong as 6.   IKE and wind and surge destructive potential ratings are now included on the NOAA-AOML Hurricane Research Division experimental research wind field products available at www.aoml.noaa.gov/hrd/data_sub/wind.html

 3. Radial extent of the surface wind field

Standardization and real-time objective analysis methods applied to measurements from diverse observation platforms tend to result in radial wind field extent estimates that exceed those conducted operationally. Recent research conducted at Penn State (Moyer et al., 2007) suggests that the extent of tropical storm force wind radii is underestimated operationally by ~ 15%. In general, the standardization corrections conducted to coastal and marine wind observations act to increase the winds from the raw values transmitted in realtime. Observing platforms to be corrected upward in wind speed include buoys with 5 m level wind measurements, coastal platforms with terrain obstructions to the flow, and remote sensing platforms that measure over relatively large footprints.

4. Behavior of the surface drag coefficient

The surface momentum flux is therefore governed by the drag or friction at the sea surface which in turn depends on a roughness which is parameterized as increasing with increasing wind speed. Measurements support this parameterization only up to wind speeds of ~28 m/s. For higher wind speeds the roughness dependence is extrapolated e.g. Large and Pond (1981). The surface enthalpy flux is also modeled using the bulk aerodynamic method and employs an enthalpy exchange coefficient that is dependent on C_D. According to the theory of Emanuel (1995), a hurricane is only maintained if kinetic energy is supplied by oceanic heat sources at a rate exceeding dissipation, suggesting a ratio of enthalpy exchange coefficient (C_E) to C_D ranging from 1.2 to 1.5 for mature hurricanes. At extreme wind speeds > 50 m/s, the typical extrapolations of wind speed dependent drag coefficients found in most models cause kinetic energy to be destroyed too rapidly to sustain a hurricane (Donelan et al., 2004).

In Powell et al., (2003), hereafter "PVR", analysis of mean profiles documented a logarithmic change of wind speed with height, suggesting the applicability of surface layer similarity in conditions associated with MBL winds up to 70 m/s. Using the "Profile Method", a fit of the profiles provided information on the surface stress or friction velocity (slope) and roughness (intercept) as a function of wind speed. The basis for the Profile method used by PVR method is that each sonde profile is a realization or snap shot of tropical cyclone conditions. By organizing numerous realizations as a function of wind speed, the ergodic hypothesis (Panofsky and Dutton 1984) is invoked to consider each profile as an instance from an ensemble of profile samples in nearly identical conditions. The primary feature controlling the turbulence in these conditions is the ocean surface roughness and this quantity is dependent on the wind stress and sea state, hence the organization by wind speed. The profiles are organized by the "mean boundary layer" wind speed, defined as the average of all values below 500 m. Profiles are filtered to remove under-sampled flow (turbulent eddies, convective- and swell-related features) and noise due to satellite switching. Averaging the profiles removes larger scale convective features such as transient wind maxima or minima and provides information on the mean state and how it changes with the wind forcing. PVR analyzed 331 GPS sondes dropped in 15 storms from 1997-1999. This analysis determined a leveling off of the surface stress and drag coefficient in wind speeds > 34 m/s and a reduction in roughness length. This was the first time that measurements of drag coefficient were made in winds > 28 m/s.

The intensive CBLAST investigations of 2003 Hurricanes Fabian and Isabel, together with experiments conducted in Hurricanes Frances, Ivan, and Jeanne of 2004 , and intensive sampling of 2005 Hurricanes Katrina, Rita, and Wilma, provide a wealth of high wind GPS sonde profile measurements to extend the work of PVR. In particular, observational determination of the spatial distribution of roughness relative to the hurricane center to account for azimuthal variation of wave age and steepness as a function of wind speed will provide a data set for validating the current model parameterizations and developing new ones. To evaluate the effect

of sea state, which varies in azimuth because of the variation in swell characteristics relative to the wind, a larger (than PVR) data set is needed, ideally containing ~150 profiles for a given MBL grouping. The GPS sonde data through 2005 provide sufficient profiles to study the azimuthal variation of surface stress and roughness.

Mean wind speed profiles were determined from the bin-average wind speeds for each MBL group. The profiles were plotted as Ln height vs. wind speed and a least squares linear regression fit eqn (5) estimated the slope (ratio of the Von Karman constant (0.4) to the friction velocity) and intercept (Zo, roughness length) for each MBL group.

$$Ln\ Z = (k/U^*)\ U + Ln\ (Zo) \tag{1}$$

$$Cd = \left(\frac{.4}{Ln\left(\frac{Zo}{10}\right)} \right)^2 \tag{2}$$

The drag coefficient was then computed from the roughness length. Since the number of samples within the lowest two bins (8-12 m and 13-19m) was typically much less than that at 20-29 m, two estimates of the surface layer quantities were estimated. One estimate for the 8-150 m surface layer, and the second for the 20-150 m surface layer. Since sea surface temperatures are not available from the sondes, no attempt was made to compute a surface layer ψ_m value associate with the departure of the wind profile from a neutral stability shape.

4.1 Cd behavior with wind speed

Surface layer friction velocity, roughness length, and drag coefficient were computed based on linear least squares fits to the 20-160 m bin-average wind speeds. The mean surface layer wind profiles are shown in Fig. 6 for five MBL wind speed groups above 30 m s^{-1}.
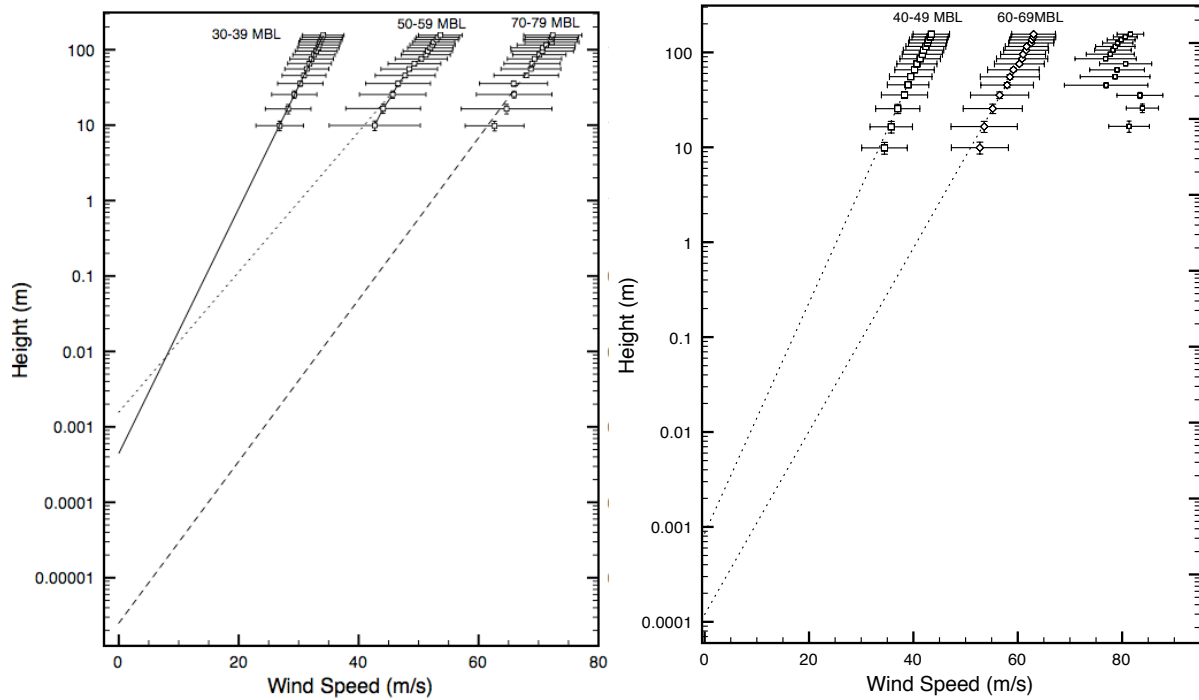
Fig. 2 Mean wind profiles by MBL group. Symbols and bars represent bin mean and standard deviation. Least squares fit lines are extended to show the roughness length associated with the Y axis intercept.

Frequently the wind speed values in the lowest two bins diverge from a line through the remaining bins indicative of winds higher than the mean fit. This behavior is not indicative of wave sheltering but rather, near-surface winds stronger than that expected from a neutral stability log law. The lines shown in Fig. 2 were based on the 20-160 m layer, which is above the layer where the points diverge from the log profile. The roughness lengths determined from the intercepts of Fig. 2 were used to compute the drag coefficients (red squares) in Fig. 8.
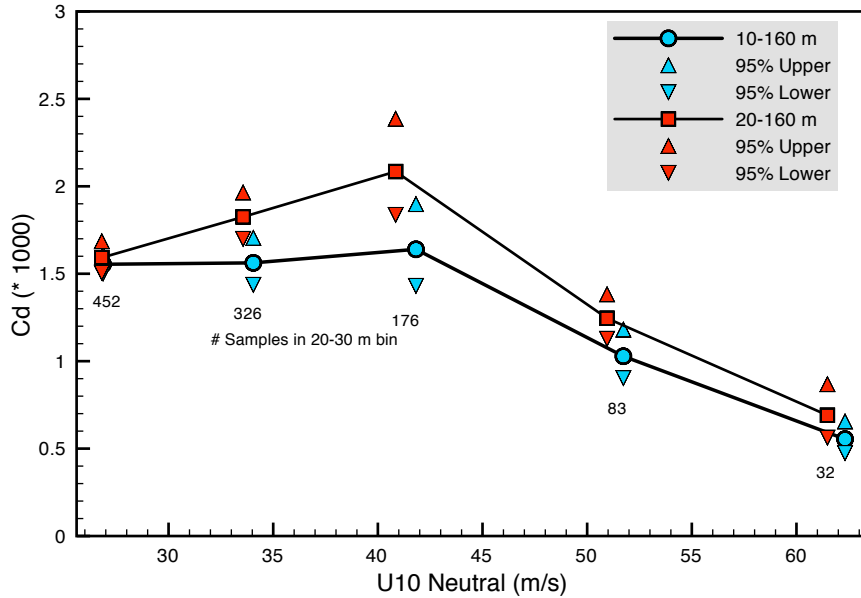
Fig. 3 Drag coefficient (squares) as a function of 10 m neutral stability wind speed. Upward and downward pointing triangles indicate the 95% confidence limits on the estimates. Numbers near each symbol indicate the number of wind speed samples in the 21-30 m bin.

Although the confidence intervals are similar with estimates based on the 10-160 m or the 20-160 m surface layers, the 20-160 m surface layer (without the 8-12 m and 13-20 m layers) have in general slightly better r^2 values and less influence from the departures of bin averages from the least squares fit line. We consider the 20-160 m layer to be more representative of the lowest levels that might be considered in mesoscale numerical prediction models such as HWRF. Drag coefficient behavior with wind speed (Fig. 3) shows a similar (to PVR, Fig. 4) initial increase with wind speed up to 10 m neutral stability wind speeds of about 42 m s^{-1}, followed by a decrease as surface winds increase to ~ 62 m s^{-1}. In comparison to PVR, the Cd values are all lower and the decrease is well defined. The large 95% confidence limits in Cd shown in PVR suggested that the Cd could either saturate or perhaps decrease, whereas these results point to a well defined decrease, and now include the 70-79 m s^{-1} MBL group. This group contained insufficient profiles to conduct analysis in PVR. Too few profiles were available to conduct analysis for the 80-89 m s^{-1} MBL group. A recent paper in BAMS by Black et al., (2007) determined Cd (Fig. 5) using the SFMR measured surface wind speed and a friction velocity estimated by extrapolation of eddy correlation flux profile estimates between 70 and 400m. A total of 42 flux legs were flown in relatively clear regions outside of the main rainband convection in six regions of stepped-descent flight patterns in Hurricane Fabian and Isabel during the CBLAST field experiment. They claim that Cd begins to decrease occurs at much lower wind speeds of 23 m s^{-1}. The CBLAST Cd estimates have relatively large confidence limits such that it is difficult to attribute a transition wind speed; our Cd at 27 m s^{-1} falls within their error limits and they have no measurements for wind speeds above 29 m s^{-1}.
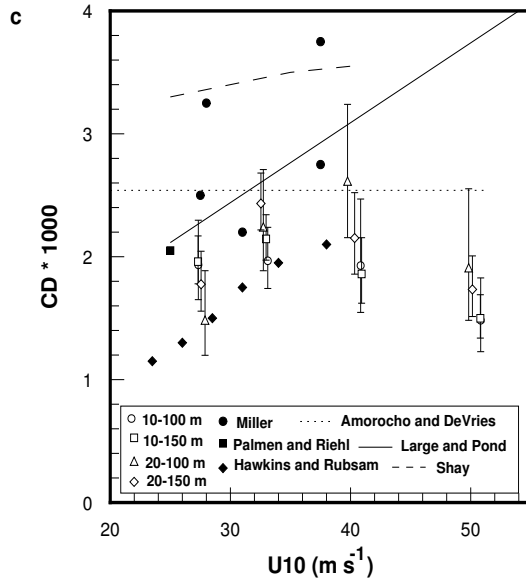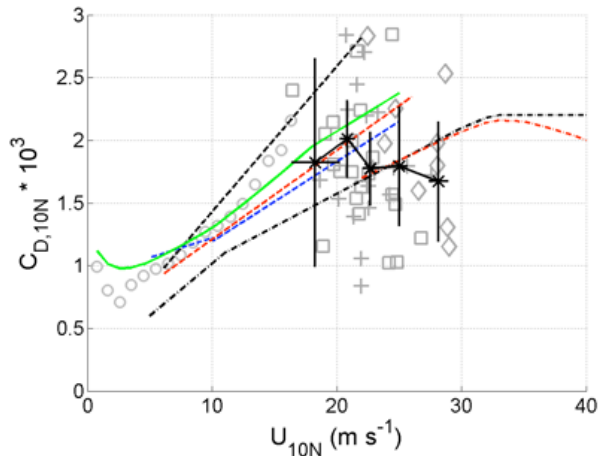
Fig. 4 Cd vs U10 from PVR

Fig. 5 Cd vs U10 from Black et al., 2007

4.2 Radial dependence of Cd

Most sondes in the MBL wind speed groups > 50 m s^{-1} were launched according to a strategy to place them radially inward from the radius of maximum wind (to attempt to sample the surface maximum wind). The median of the radial distance of the drops in MBL groups > 50 m s^{-1} is near 30 km and we use this as a criterion for examining radial dependence of the mean wind profiles.   It is advantageous to look at the mean profiles as a function of the actual radius rather than a scaled radial coordinate. A scaled coordinate would combine large and small storms together whereas, Kepert (2001, 2006) has shown that the curvature of the flow (in how it relates to inertial stability and relative angular momentum) is an important factor in the location and

strength of boundary layer jets. A fixed radius of 30 km was selected to examine the dependence of the mean wind profile and surface layer characteristics at small and large radii.

Cd values determined from mean wind profiles < 30 km from the storm center (Fig. 6a) have fewer samples (due to the majority of profiles in the 30-39 and 40-49 m s^{-1}) with lower magnitudes and are relatively insensitive to changes in wind speed. Cd determined from profiles beyond 30 km (Fig. 6b) show a more pronounced increase with wind speed up to about 40 m s^{-1} followed by a sharp decrease at higher winds (although few samples are contained in the 70-79 MBL group estimates at surface winds of about 60 m s^{-1}). While Rmax data are not yet available for all drops, it is likely that the profiles < 30 km are also radially inward from Rmax. The mean wind profile at small radii is associated with flow trajectories having greater curvature such that "new" waves are always in a state of development and the sea state is characterized by the continuous breaking mechanism hypothesized by Donelan 2004. At larger radii with smaller trajectory curvature, the mean wind profile may be more influenced by interactions with waves that are in a more developed state.
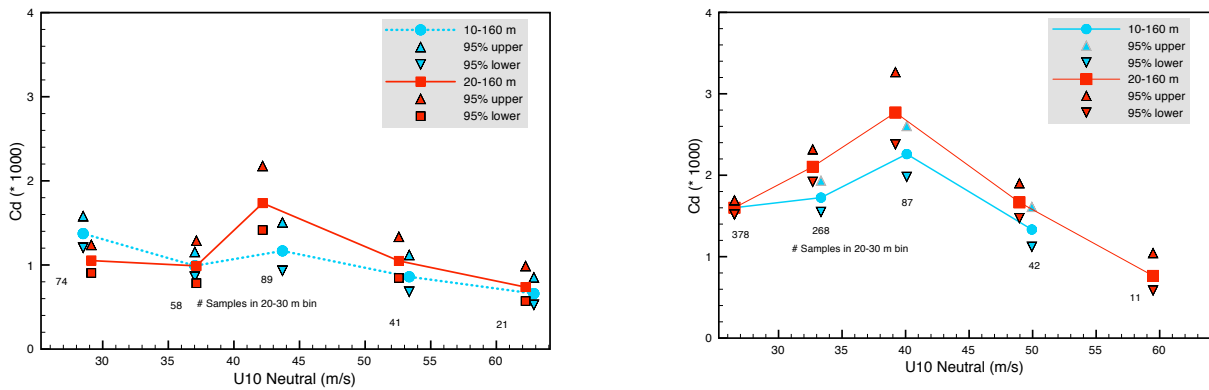

Fig. 6 Cd vs U10 a) less than 30 km radial distance (top), b) > 30 km radius (bottom).

4.3 Cd Variation with Storm-relative Azimuth

Results of the previous section indicate that region beyond 30 km radial distance is most likely to show an azimuthal signal in Cd behavior and this breakdown of the data have sufficient samples for further binning by storm relative azimuth. Indeed an important objective of this project is to investigate the azimuthal dependence of the drag coefficient. As depicted by this plot from Wright et al and Ed Walsh's scanning radar altimeter wave data (Fig. 1) superimposed on an H*Wind analysis of Hurricane Bonnie of 1998, we can divide a storm into three regions (Black et al., 2007): 1) Rear sector (151-240 degrees relative to the storm motion vector) with 150-200 m long waves moving with the wind, 2) Right sector (21-150 degrees) with 200-300 m long waves moving outward by up to 45 degrees relative to the wind, and 3) Left front sector (241-020 degrees) where 300 m long waves travel outward at 60-90 degrees to the wind.
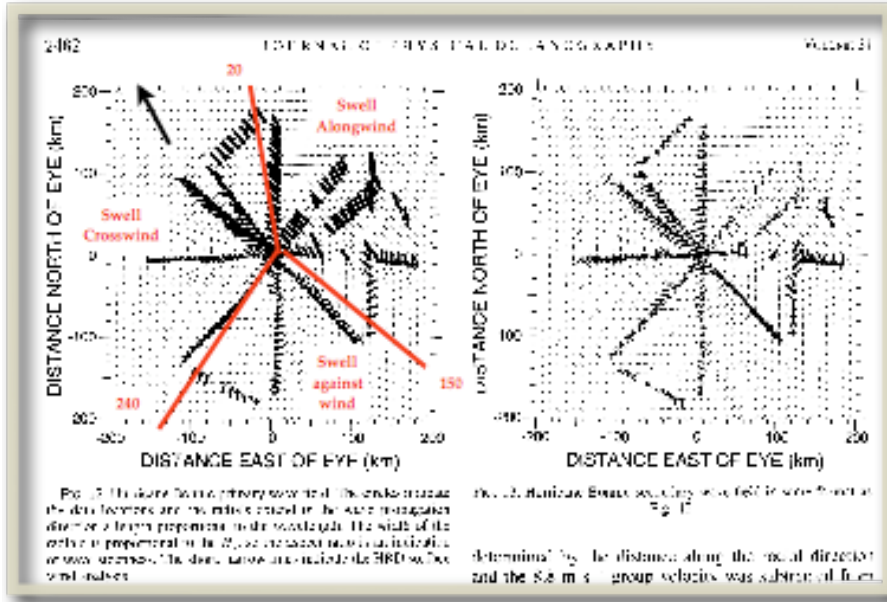
Figure 7. from Wright et al., 2001 showing wave and wind field for Hurricane Bonnie.

In the rear sector (151-240 degrees) where the waves tend to move in the same direction as the wind, Cd is relatively constant and then decreases for winds above 34 m s^{-1} (Fig. 8). In the front left sector (241-020 degrees) the increase with wind speed behavior is very well defined with a maximum at winds of about 36 m s^{-1} and Cd values up to 4.7 x 10^{-3}, followed by a rapid decrease as wind increase above 37 m s^{-1}. In this sector the primary wave field moves crosswind as depicted in Fig. 7. For comparison, the data are superimposed in Fig. 8.
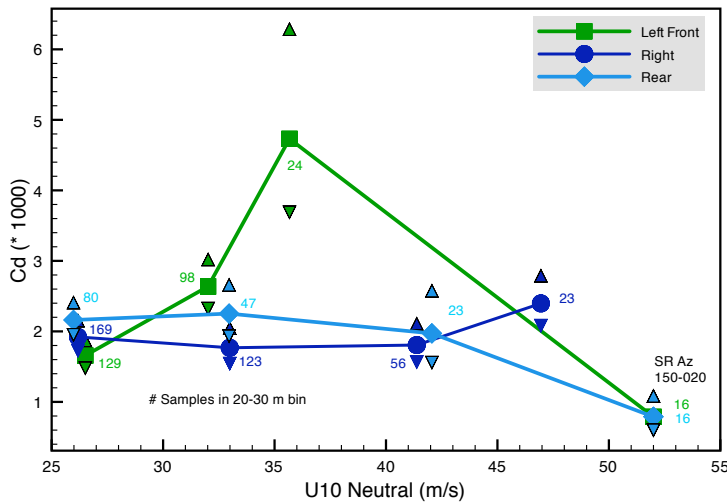

Fig. 8 Cd vs U10 for radius > 30 km summarizing results for the 20-160 m surface layer..

These results suggest that Cd is most sensitive to wind speed in the left front sector, where scanning radar altimeter data suggest the waves have the longest wavelengths and tend to move outward 60-90 degrees crosswind. Data were insufficient to establish Cd behavior for the 70-79

m s^{-1} MBL group. While the long wavelength waves resolved by the scanning radar altimeter are not directly relevant to the surface stress (associated with smaller high-frequency wind waves), the outward moving long period waves in the left front may modulate the wind wave field such that larger roughness elements are present. The sea state condition caused by smaller wind waves interacting with a fast swell moving outward crosswind, is apparently associated with larger surface roughness than found elsewhere in the storm. This condition is corroborated by examination of the Stepped Frequency Microwave Radiometer (SFMR) - GPS sonde difference pairs as a function of storm relative azimuth in a recent paper by Uhlhorn and Black (2003) and an updated version of their plot using 416 SFMR-GPS sonde pairs by Powell et al., 2007 (manuscript in preparation), reproduced in Fig. 9. This fit is used to correct the SFMR (which responds to emission from sea foam) for non-wind sources of roughness related to storm regions where wind seas are in the developing stage (more energy going into building the sea than being dissipated). In the right-rear the swell and wind are going in the same direction so the swell is growing and leaving less foam due to fewer breaking waves (hence negative differences), while on the left front side the swells are generally propagating across the wind, leading to more breaking and more foam than wind seas alone (positive differences).
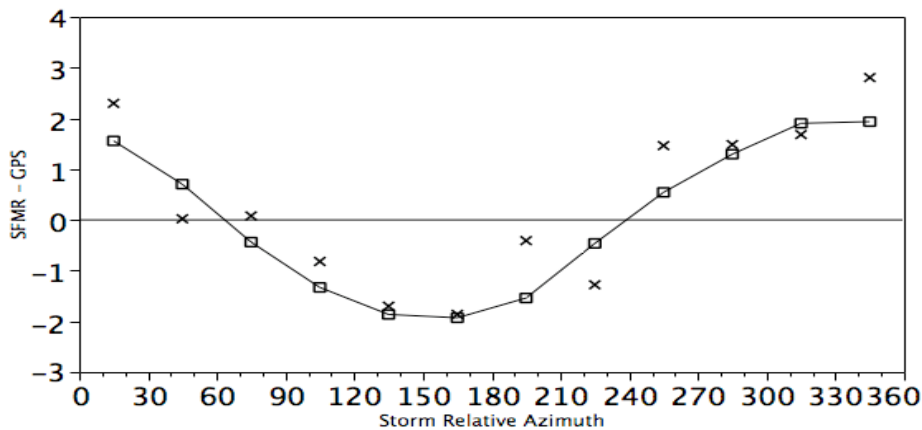

Fig. 9 SFMR-GPS sonde surface wind speed difference as a function of storm-relative azimuth.

4.4 Discussion

Surface layer quantities were estimated from five mean wind profiles spanning MBL winds of 30-79 m s^{-1} and 10 m level neutral stability winds of 26-62 m s^{-1}. All mean wind profiles but the 30-39 MBL exhibit kinks within 20 m of the surface such that some process must be allowing a stronger wind than expected from the log law, close to the surface. Arguments associated with wave sheltering would be associated with a kink in the wind profile in the opposite direction than that observed. Shallow unstable layers associated with relatively cool air over warm water, though observed, are unlikely as a primary mechanism since the instability would lead to greater vertical mixing, a condition that would inhibit profile kinks. A shallow stable layer with relatively warm air over a cooler sea surface could support a kink that would show increased shear, but such a kink would be in the opposite direction. The most likely explanation would be

interfacial properties that allow the flow in the lower two bins to be accelerated relative to flow over a more "normal" sea surface. This process would operate in the presence of shear and vertical velocity fluctuations that tend to well-mix the lower layers. Significant vertical motions are present at the lowest levels as shown in Fig. 10 for the 40-49 MBL group, and in the mean the vertical velocities are positive. The presence of generally positive vertical velocities is probably due to a combination of mesoscale forced upward motion associated with horizontal convergence, together with the buoyant plumes where relatively cool air overlies warm water.
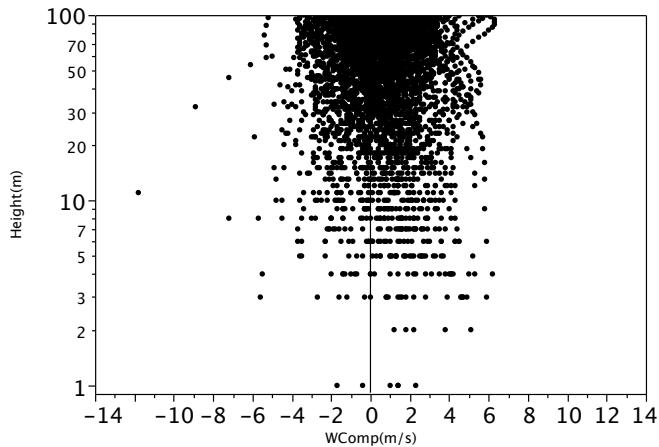

Fig. 10 Vertical component of the wind speed as a function of height for the 40-49 MBL group.

A likely mechanism for the wind profile kinks would be the interfacial property of sea foam. PVR presented photographic evidence supporting enhanced sea foam coverage when winds are > 40 m s^{-1}. They speculated that the surface properties of a sea foam emulsion could promote more of a "slip" surface than a water surface. Andreas (2004) cited an obscure paper by Schmelzer and Schmelzer 2003 finding that bubble layers have lower surface tension and tensile strength than a water surface, hence a bubble layer would have difficulty supporting small-scale capillary waves that are thought to support stress at the sea surface. Andreas also speculated that spume and sea spray droplets support much of the stress near the ocean surface resulting in (assuming the total stress in the surface layer is constant with height) a decrease in stress supported by the air. He also suggested that sea spray and rain help to flatten the sea state and reduce roughness.

The foam mechanism may help to explain the relatively small Cd values within 30 km of the storm. In this location we speculate that the continuous breaking process described by Donelan 2004 together with the resultant foam layer, is the predominant mechanism leading to reduced Cd over a wide range of wind speeds. At radii beyond 30 km, the surface roughness is greatest and show the most sensitivity to wind in the left front quadrant where the swell propagates crosswind. There is a contradiction of processes in this quadrant since the crosswind swell promotes wave breaking and enhanced foam coverage but we also see the highest Cd values anywhere in the storm in this region. Our results suggest that in the left front sector, the interaction of the local wind waves with long-period, outward-propagating, crosswind swells

contributes to higher roughness and that despite indications of enhanced foam coverage, the scale of wave breaking is not sufficient to reduce the roughness until the winds exceed 36 m s^{-1}.

The results from PVR and Donelan 2004 have motivated the modeling community to experiment with new parameterizations for the surface drag. Additional field results have corroborated the findings in PVR. Examples of Cd parameterizations include Chen et al., 2007 and Moon et al., 2004a,b. These approaches include "capping" Cd at some value when winds exceed hurricane force speeds. The 95% confidence limits on the PVR estimates of Cd were too large to determine whether Cd saturated or decreased at extreme wind speeds. Now, with nearly 3 times the number of profiles, we have found that Cd indeed decreases in extreme winds. Recent independent oceanographic measurements in hurricanes support our finding (Shay and Jacob 2006, Jarosz et al., 2007). The behavior of Cd with wind speed is more complicated than a simple capping with wind speed but depends on location relative to the storm. We encourage modelers to experiment with parameterizations that allow Cd-wind behavior to vary by radial distance and storm relative azimuth. In idealized hurricane experiments with a couple wind-wave model , Moon et al., (2004b) found that the higher, longer, more fully developed waves in the right and front of the storm yielded older wave ages with higher values of Cd while lower shorter and younger waves to the rear and left yielded lower drag coefficients. In light of the inconsistencies with the findings reported here, further modeling investigations are warranted.

Acknowledgements

References

Andreas, E.L., 2004: Spray stress revisited. *J. Phys. Ocean.,* 34, 1429-1439.

Black, P. G. and coauthors, 2007: Air-sea exchange in hurricanes: Synthesis of observations from the Coupled Boundary Layer Air-Sea Transfer experiment. *Bull. Amer. Meteor. Soc.*, 88, 357-374.

Bender, M. A., I. Ginis, and Y. Kurihara, 1993: Numerical simulations of tropical cyclones-Ocean interaction with a high-resolution coupled model. *J. Geophys. Res.*, 98, 23245-23263.

Chen S.S. and coauthors, 2007: The CBLAST-hurricane porogram and the next-generation fully coupled atmosphere-wave-ocean models for hurricane research and prediction., *Bull. Amer. Meteor. Soc.*, 88,311-317.

Donelan, M. A. B. K. Haus, N. Reul, W. Plant, M. Stiassnie, H. Graber, O. Brown, and E. Saltzman, 2004: On the limiting aerodynamic roughness of the ocean in very strong winds. *Geophys. Res. Lett*, 31, L18306.

Emanuel, K.A., 1995: Sensitivity of tropical cyclones to surface exchange coefficients and a revised steady-state model incorporating eye dynamics. J. Atmos. Sci., 52, 3969-3976.

Hock, T.F. and J. L. Franklin, 1999: The NCAR GPS dropsonde . Bull. Amer. Meteor. Soc., 80, 407-420.

Jarosz, E., D. A. Mitchell, W. W. Wang, and W. J. Teague, 2007: Bottom-up determination of air-sea momentum exchange under a major tropical cyclone. *Science*, **315**, 1707-1709.

Kepert, J.D., 2001: The dynamics of boundary layer jets within the tropical cyclone core. Part I: Linear theory. J. Atmos. Sci., 58, 2469-2484.

Kepert, J. D., 2006: Observed boundary layer wind structure and balance in the hurricane core. Part I: Hurricane Georges. J. Atmos. Sci., 63, 2169-2193.

Kepert, J. D., 2006: Observed boundary layer wind structure and balance in the hurricane core. Part II: Hurricane Mitch. J. Atmos. Sci., 63, 2194-2211.

Large, W.G., and S. Pond, 1981: Open ocean momentum flux measurements in moderate to strong winds. *J. Phys. Oceanogr.*, 11**,** 324-336.

Moon, I. J., I. Ginis, and T. Hara, 2004: Effect of surface waves on Charnock coefficient under tropical cyclones., *Geophys. Res. Lett*, 31, L20302.

Moon, I. J., I. Ginis, and T. Hara, 2004:Effect of surface waves on air-sea momentum exchange. Part II Drag coefficient under tropical cyclones., J. Atmos. Sci., 2334-2348.

Panofsky, H. A. and J. A. Dutton, 1984: Atmospheric turbulence: Models and methods for engineering applications. John Wiley and Sons, N. Y., 397 pp. 397.

Powell, M. D., P. J. Vickery, and T. Reinhold, 2003: Reduced drag coefficient for high wind speeds in tropical cyclones. *Nature*, 422, 279-283.

Shay, L.K. and S. D. Jacob 2006: Relationship between oceanic energy fluxes and surface winds during tropical cyclone passage. Atmosphere-Ocean Interactions Volume II, Advances in Fluid mechanics, 115-142.

Uhlhorn, E. and P. G. Black, 2003: Verification of remotely sensed sea surface winds in hurricanes. J. Atmos and Ocean Tech., 20, 99-116.

Walsh, E. J., others, M. D. Powell, Black, and F. D Marks, Jr., 2002: Hurricane directional wave spectrum spatial variation at landfall. *J. Physical Ocean*., **32**, 1667-1684.

 Wright, C.W., others, M.D. Powell, Black, and Marks, 2001: Hurricane directional wave spectrum spatial variation in the open ocean. *J. Phys. Ocean*., **31**, 2472-2488.